Magnonic beam splitter: The building block of parallel magnonic circuitry

A. V. Sadovnikov, C. S. Davies, S. V. Grishin, V. V. Kruglyak, D. V. Romanenko, Yu. P. Sharaevskii, and S. A. Nikitov

Citation: Applied Physics Letters **106**, 192406 (2015); doi: 10.1063/1.4921206

View online: http://dx.doi.org/10.1063/1.4921206

View Table of Contents: http://scitation.aip.org/content/aip/journal/apl/106/19?ver=pdfcov

Published by the AIP Publishing

Magnonic beam splitter: The building block of parallel magnonic circuitry

A. V. Sadovnikov,[1] C. S. Davies,[2] S. V. Grishin,[1,a)] V. V. Kruglyak,[2] D. V. Romanenko,[1] Yu. P. Sharaevskii,[1] and S. A. Nikitov[1,3]
[1]*Laboratory "Metamaterials," Saratov State University, Saratov 410012, Russia*
[2]*School of Physics, University of Exeter, Stocker Road, Exeter EX4 4QL, United Kingdom*
[3]*Kotel'nikov Institute of Radioengineering and Electronics, Russian Academy of Science, Moscow 125009, Russia*

(Received 5 February 2015; accepted 2 May 2015; published online 13 May 2015)

We demonstrate a magnonic beam splitter that works by inter-converting magnetostatic surface and backward-volume spin waves propagating in orthogonal sections of a T-shaped yttrium iron garnet structure. The inter-conversion is enabled by the overlap of the surface and volume spin wave bands. This overlap results from the demagnetising field induced along the transversely magnetised section(-s) of the structure and the quantization of the transverse wave number of the propagating spin waves (which are therefore better described as waveguide modes). In agreement with numerical micromagnetic simulations, our Brillouin light scattering imaging experiments reveal that, depending on the frequency, the incident fundamental waveguide magnonic modes may also be converted into higher order waveguide modes. The magnonic beam splitter demonstrated here is an important step towards the development of parallel logic circuitry of magnonics. © *2015 AIP Publishing LLC*. [http://dx.doi.org/10.1063/1.4921206]

The field of magnonics offers the prospect of a technology that could complement and possibly supersede conventional electronics.[1,2] As such, a tremendous amount of research has been devoted in recent years to the development of spin-wave based technology, and many milestones have already been reached, with the realization of spin wave logic gates,[3–5] filters,[6] delay lines,[7] and multiplexors,[8] for example. Whilst the design of the aforementioned building blocks of magnonic circuits is indeed very important, it is an open question as to how they could be linked together in parallel, so that the devices could collectively perform increasingly complex computational tasks. The building block of electronic parallel circuits is the splitter (a T-junction of conducting wires). In this circuit element, an electrical current is directed along the "leg," whereupon it is then split and channelled along both "arms." To drive and control currents across the circuit, electronics relies on the electric potential delivered by a voltage source. This quantity is immune to twists and steers of the conducting wires, and so an electronic splitter is straightforward to construct and understand. Magnonics, however, has no analogous driving mechanism. The design of a magnonic beam splitter is therefore an important first step towards the construction of parallel magnonic circuits.

From the magnetostatic spin wave (MSW) theory[9,10] developed for ferrite media with finite thickness and infinite in-plane dimensions, it is well-known that the anisotropic MSW dispersion can be controlled by the strength and orientation of the external bias magnetic field $\boldsymbol{H}_0$. With the bias field and the spin-wave wave vector $\boldsymbol{k}$ both directed in-plane, two types of spin waves can exist. If $\boldsymbol{k}$ is orthogonal/parallel to $\boldsymbol{H}_0$, magnetostatic surface spin waves (MSSWs)/backward-volume MSWs (BVMSWs) propagate. These two spin-wave types exist in distinct frequency ranges extending above (for MSSWs) and below (for BVMSWs) a common cut-off frequency equal to the frequency of ferromagnetic resonance f_{FMR}.[11] This is defined by $f_{FMR} = \sqrt{f_H(f_H + f_M)}$, with $f_H = \gamma|\boldsymbol{H}_i|$ and $f_M = 4\pi\gamma M_0$, where γ is the electronic gyromagnetic ratio (2.80 MHz/Oe), $\boldsymbol{H}_i$ is the internal magnetic field, and M_0 is the magnetization of saturation.

Several significant investigations[12–15] have already explored the consequences of lateral confinement on the features of propagating spin waves. In particular, Brächer *et al.*[15] studies a T-junction of magnonic waveguides, albeit with functionality reversed to that investigated here. Generally, the lateral confinement within magnonic waveguides gives rise to two effects. First, the transverse wave number becomes quantized, leading to the formation of width (waveguide) modes in both MSSW and BVMSW configurations.[16] Second, the in-plane demagnetizing field ("shape anisotropy") introduced by the waveguide edges reduces the internal field in the MSSW configuration[15] and therefore similarly reduces the frequency of ferromagnetic resonance. These two effects lead to overlap in the frequency bands of MSSWs and BVMSWs. In their study, Brächer *et al*. exploited these two effects to realise a magnonic beam combiner element. Counter-propagating MSSW modes were initially excited at both ends of the T-junction's arms, with the bias field directed in-plane but orthogonal to the T-junction's arms, i.e., parallel to its leg. Upon interfering, Brächer *et al*. observed the MSSW modes combining to form a BVMSW width-mode propagating along the leg of the T-junction. By tuning the frequency (and hence wavelength) of the interfering MSSW modes, the order of the output BVMSW mode could be controlled.

Here, we demonstrate that the dispersion overlap inherent to rectangular waveguides can be used to interconvert spin waves reciprocally between the MSSW and BVMSW geometries within a dielectric magnonic beam splitter structure. First, all-electrical microwave transmission measurements are

a)Electronic mail: grishfam@sgu.ru

used to select magnonic waveguides that are sufficiently narrow to feature the dispersion overlap. Then, Brillouin light scattering (BLS) imaging is used to demonstrate the functionality of the device in different frequency regimes. In both cases, micromagnetic simulations are used to validate the experimental observations and to reveal the mode structure of the spin-wave beam in the different parts of the magnonic beam splitter.

The investigated yttrium-iron-garnet (YIG) waveguides (Figs. 1(a) and 1(b)) with thickness of $s = 7.7\,\mu$m and width of either $w = 3$ mm or 0.5 mm were fabricated by laser scribing a continuous YIG film epitaxially grown on a substrate of gadolinium gallium garnet (GGG). The waveguides were initially magnetized by a uniform in-plane bias field $H_0 = 1225$ Oe, directed along either the long or short symmetry axis of the waveguide. Spin wave transmission characteristics were acquired using two 30 μm wide microstrip antennas positioned on either end of the waveguides. The input antenna's dynamic magnetic field couples to the YIG's magnetization, exciting spin waves propagating along the waveguide. The efficiency of spin wave propagation was measured using a vector-network-analyser. The distributions of the projection of the magnetization on to the internal field, across the width of the waveguides, were modelled using micro-magnetic simulations performed with the Object-Oriented Micro-Magnetic Framework (OOMMF).[17,18] We approximated the waveguide as a cuboid of size $(600 \times w \times 0.0077)$ mm^3 with a cell-size of $(10 \times 0.05 \times 7.7)\,\mu$m^3. One-dimensional periodic boundary conditions[19] were implemented along the waveguide's long axis, and the exchange interaction was neglected (due to the dominance of the Zeeman and demagnetizing energies). We assumed $4\pi\gamma M_0 = 1750\,G$ and neglected any crystalline anisotropy energy.

The results from the initial characterisation of the waveguides are shown in Fig. 2. For a waveguide width of 3 mm (Fig. 2(a)), the MSSW and BVMSW transmission spectra do not overlap and have a common cut-off frequency at $f_\perp = 5.345$ GHz. Since $f_{FMR} = 5.345\,\text{GHz} = f_\perp$, the 3 mm wide waveguide can be considered a continuous film. Upon reducing the waveguide width to 0.5 mm (Fig. 2(b)), the upper cut-off frequency of the BVMSW spectra remains at 5.345 GHz,

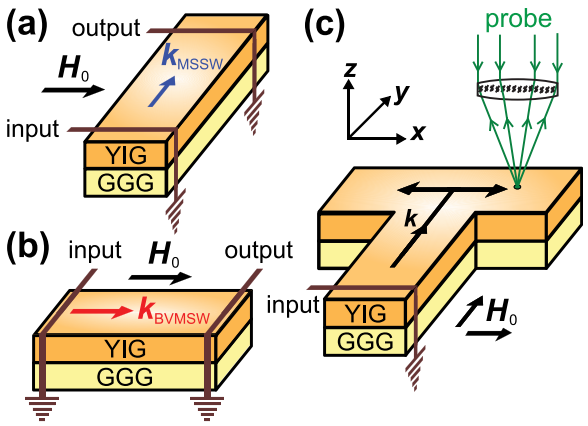

FIG. 1. (a) and (b) Schematics of the ferromagnetic waveguide elements in the MSSW and BVMSW configurations respectively. (c) By coupling the two orthogonal waveguides, we obtain a splitter geometry.

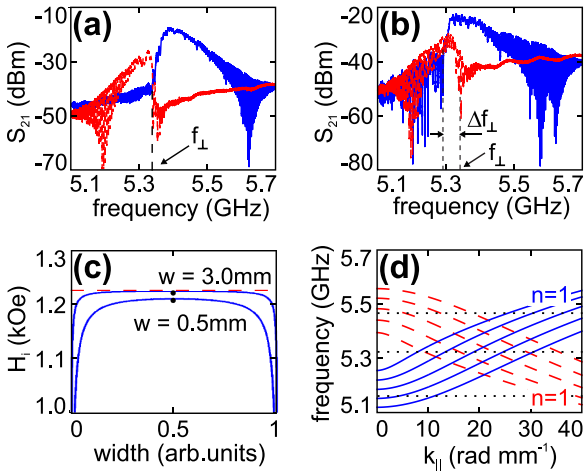

FIG. 2. (a) and (b) Transmission characteristics S_{21} of the YIG waveguides, measured in the MSSW (solid-blue line) and BVMSW (dashed-red line) configurations, with a waveguide width $w = 3$ mm and 0.5 mm, respectively. (c) Calculated distributions of the static internal magnetic field across the normalized width of the waveguide for the different MSW configurations. (d) Analytically calculated dispersion curves for the longitudinal wave vector $k_{||}$ of the MSW width modes. The curves are in order of increasing integer values of n, ranging between $n = 1$ to $n = 5$ for both MSSW and BVMSW configurations.

but the MSSW band's lower cut-off is reduced by 114 MHz and is equal to 5.231 GHz. The experimental overlap between the MSSW and BVMSW bands is therefore $\Delta f_\perp = 114$ MHz. This overlap is partially explained by the static internal field profiles presented in Fig. 2(c). When the waveguide width is 3 mm, the internal field at the centre of the waveguide is 1222 Oe in the MSSW configuration, whereas reducing the width to 0.5 mm reduces the field strength to 1208 Oe. This field variation corresponds to a frequency shift of 39.2 MHz. In addition to this, we must consider the effect introduced by lateral quantization, whereby the component of the spin-wave wave vector, orthogonal to the waveguide's longitudinal axis, must satisfy $k_\perp = \frac{n\pi}{w_{eff}}$ (where n is an integer and w_{eff} is the "effective" width of the waveguide). Here, we have assumed the magnetization at the edges of the waveguide to be partially pinned,[20] where the waveguide modes have an effective width of 0.525 mm. This leads to frequency-offset spin wave dispersions for the different waveguide width-modes as calculated[21] and shown in Fig. 2(d). The analytical frequency overlap between the $n = 1$ modes is 139 MHz, which is within 22% of the experimentally measured value of 114 MHz.

There are three additional points of note relating to the dispersions of the different spin wave width-modes. First, the efficiency of exciting the width-modes decreases as n increases. Increasing the number of nodes across the waveguide width therefore reduces the net torque that can be exerted by the exciting field. Second, only odd width modes ($n = 1, 3, 5\ldots$) can be excited by a microstrip antenna, as even modes have no net magnetic moment across the waveguide width, so no coupling with a homogeneous dynamic field can occur.[22] Third, we have run further simulations to identify the origin of the discrepancy that remains between the experimentally-measured and analytically-calculated values for $\Delta f_\perp$ (114 MHz and 139 MHz respectively). Given in the supplementary material[23] are the spin wave dispersion profiles across the waveguides, calculated using the results

of micromagnetic calculations. The overlap calculated using micromagnetic calculations is found to be 133 MHz, which is much closer to the analytically calculated value. We therefore deduce that the discrepancy between the experimentally measured and analytically calculated values for $\Delta f_\perp$ arises from our use of assumed simulation parameters (e.g., no roughness, zero crystalline anisotropy, etc.).

The observed overlap between the MSSW and BVMSW dispersions suggests that spin waves should be able to directly convert between the two dispersion types as they propagate across a T-shaped junction of finite width waveguides, thereby producing a magnonic beam splitter. In order to test this hypothesis, we prepared such a structure (Fig. 1(c)) using waveguides with the same width of 0.5 mm. The input antenna was positioned at the base of the T-junction's leg. The repetition interval of the pulsing microwave signal was set to 1 μs to prevent overheating, and its amplitude was fixed at -30 dBm so as to only excite linear magnetization dynamics. BLS microscopy[16] was used to image the propagating spin waves. A laser beam, of wavelength 532 nm, was focussed to a spot of diameter 20 μm on the surface of the YIG structure. As a result of inelastic scattering by the dynamic magnetization $\boldsymbol{m}$, the intensity I of the scattered light varies according to $I(x,y,t) \sim |\boldsymbol{m}(x,y,t)|^2$. The measured signal was also modelled using OOMMF to obtain in addition phase-resolved information. In these simulations, the splitter was enclosed in a $6.5 \times 2.5 \times 0.0077\,\text{mm}^3$ box, with a cell-size of $10 \times 10 \times 1.54\ \mu\text{m}^3$. Once a ground state magnetic configuration was established, spin waves were excited at the base of the T-junction's leg by a harmonic field. This dynamic field, of frequency f, was spatially distributed so as to mimic the field generated by a microstrip.[24]

Presented in the upper panels of Fig. 3 are logarithmically scaled BLS maps, measured for the two orthogonal bias field orientations relative to the splitter's leg. Both BLS measurements in Figs. 3(a) and 3(b) were performed at a frequency of 5.32 GHz, which lies between the MSSW and BVMSW $n=1$ modal dispersions (as indicated by the middle dotted line in Fig. 2(d)). In both configurations, we clearly observe the initial propagation of a spin wave along the leg of the splitter, and then the turn of the spin wave as it enters, and then propagates along both arms. Shown in the middle panels of Fig. 3 are simulated snapshots of the square of the dynamic magnetization, plotted to provide direct comparison with the distributions measured experimentally. In the lower panels of Fig. 3, the out-of-plane component of magnetization is shown, in order to obtain phase resolution. In the splitter's leg, the mode profile in the MSSW and BVMSW configurations is clearly that of the fundamental mode ($n=1$). From the asymmetry of the spin wave amplitude profile in the splitter's arms, however, we deduce that one-to-many mode splitting[25,26] has taken place, whereby an asymmetric $n=2$ mode is propagating alongside the original fundamental mode. This is in agreement with the findings of Clausen *et al.*[22]

The significance of the dispersion overlap for achieving spin wave splitting is verified by the measurements presented in Figs. 3(c) and 3(d). Here, the frequencies of excitation and detection are moved away from $f_\perp$, to the upper and lower dotted frequencies shown in Fig. 2(d). At

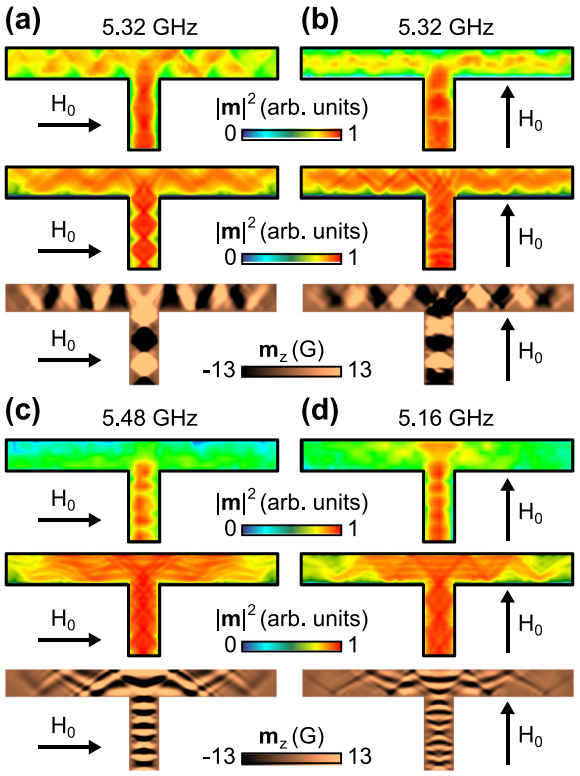

FIG. 3. Amplitude-resolved BLS maps (upper panels), simulated BLS-like maps (middle panels), and simulated snapshots of the out-of-plane component of magnetization (lower panels). (a)–(d) The spin wave propagation is mapped with the frequency and bias orientation indicated.

$f=5.48$ GHz (Fig. 3(c)), MSSW propagation is experimentally observed in the splitter's leg, but minimal propagation is observed in the arms. Similarly, in Fig. 3(d), at $f=5.16$ GHz, BVMSW propagation is seen in the leg, but there is negligible splitting. At the frequencies of 5.16 GHz or 5.48 GHz, it is impossible to limit the conversion between the BVMSW and MSSW to $n=1$ modes, since the dispersions do not overlap (Fig. 2(d)). Instead, the initial $n=1$ mode splits into $n\geq 3$ modes, which in the experiment appears to be highly inefficient. The simulations reveal that the spin wave beam in the splitter's arms is a superposition of the modes with n between 3 and 5. Further simulations, not shown here, confirm that the splitting observed in simulation is independent of the microstrip position and excitation amplitude. The reduced distance across which the split spin waves propagate is explained by the reduced dispersion gradient (i.e., group velocity) of the higher order width modes.

Let us discuss some more general matters related to the parallel magnonic circuitry. So far we have demonstrated that a T-junction of waveguides with uniform width can be used as a magnonic beam splitter within a certain frequency range. By altering the bias field strength, it is possible to adjust the splitter's frequency range of operation, as would be expected from the Kittel relation.[11] An important consideration for the development of parallel technology is the damping of spin waves, as this will restrict the extent of parallel circuits. YIG is renowned for its extraordinarily low spin wave damping, and so YIG is well-suited for this design. Although our results are obtained on length scales of

100 s of micrometres, due to the resolution of BLS, it should be possible to downscale our findings towards at least the micrometre scale.[27] Beyond this, the isotropic exchange interaction will become increasingly important,[21] which might however make the task of wave splitting simpler.[18]

In conclusion, we have demonstrated a device that can be used to split the spin wave beam within a magnonic circuit. The splitting occurs by way of inter-conversion of waveguide modes of different characters (i.e., BVMSW and MSSW types) and of different order (i.e., with different mode numbers). Micromagnetic simulations reveal that the spin wave beams in the outputs of the splitter are generally given by a superposition of both even and odd modes, with the details dictated by the dispersion overlap. By adjusting the frequency of the incident wave, it is possible to alter the character of the output beams or to switch the output off completely. Our findings are an important step towards the future parallel logic circuitry of magnonics.

The research leading to these results has received funding from the Russian Foundation for Basic Research (Project No. 14-07-00273), the Grant from Russian Science Foundation (Project No. 14-19-00760), the Scholarship of the President of Russian Federation (SP-313.2015.5), and from the Engineering and Physical Sciences Research Council of the United Kingdom (Project Nos. EP/L019876/1 and EP/P505526/1).

[1]V. V. Kruglyak, S. O. Demokritov, and D. Grundler, J. Phys. D: Appl. Phys. **43**, 264001 (2010).
[2]See http://www.itrs.net/Links/2013ITRS/Summary2013.htm on International Technology Roadmap for Semiconductors (ITRS), 2013 Edition: Emerging Research Devices.
[3]A. Khitun, B. Mingqiang, and K. L. Wang, J. Phys. D: Appl. Phys. **43**, 264005 (2010).
[4]K.-S. Lee and S.-K. Kim, J. Appl. Phys. **104**, 053909 (2008).
[5]S. V. Vasiliev, V. V. Kruglyak, M. L. Sokolovskii, and A. N. Kuchko, J. Appl. Phys. **101**, 113919 (2007).
[6]S.-K. Kim, K.-S. Lee, and D.-S. Han, Appl. Phys. Lett. **95**, 082507 (2009).
[7]V. Y. Kobljanskyj, G. A. Melkov, V. M. Pan, V. S. Tiberkevich, and A. N. Slavin, IEEE Trans. Magn. **38**, 3102 (2002).
[8]K. Vogt, F. Y. Fradin, J. E. Pearson, T. Sebastian, S. D. Bader, B. Hillebrands, A. Hoffmann, and H. Schultheiss, Nat. Commun. **5**, 3727 (2014).
[9]R. W. Damon and J. Eschbach, J. Phys. Chem. Solids **19**, 308 (1961).
[10]A. G. Gurevich and G. A. Melkov, *Magnetization Oscillations and Waves* (CRC-Press, London, New York, 1996).
[11]C. Kittel, J. Phys. Radium **12**, 291–302 (1951).
[12]T. W. O'Keeffe and R. W. Patterson, J. Appl. Phys. **49**, 4886 (1978).
[13]*Spin Wave Confinement*, edited by S. O. Demokritov (Pan Stanford Publishing Ltd., 2009).
[14]J. Jorzick, S. O. Demokritov, B. Hillebrands, M. Bailleul, C. Fermon, K. Y. Guslienko, A. N. Slavin, D. V. Berkov, and N. L. Gorn, Phys. Rev. Lett. **88**, 047204 (2002).
[15]T. Brächer, P. Pirro, J. Westermann, T. Sebastian, B. Lägel, B. Van de Wiele, A. Vansteenkiste, and B. Hillebrands, Appl. Phys. Lett. **102**, 132411 (2013).
[16]S. O. Demokritov, B. Hillebrands, and A. N. Slavin, Phys. Rep. **348**, 441 (2001).
[17]M. Donahue and D. Porter, *Interagency Report NISTIR 6376* (NIST, Gaithersburg, MD, 1999).
[18]M. Dvornik, Y. Au, and V. V. Kruglyak, Top. Appl. Phys. **125**, 101 (2013).
[19]K. M. Lebecki, M. J. Donahue, and M. W. Gutowski, J. Phys. D: Appl. Phys. **41**, 175005 (2008).
[20]K. Y. Guslienko, S. O. Demokritov, B. Hillebrands, and A. N. Slavin, Phys. Rev. B **66**, 132402 (2002).
[21]B. A. Kalinikos and A. N. Slavin, J. Phys. C **19**, 7013 (1986).
[22]P. Clausen, K. Vogt, H. Schultheiss, S. Schäfer, B. Obry, G. Wolf, P. Pirro, B. Leven, and B. Hillebrands, Appl. Phys. Lett. **99**, 162505 (2011).
[23]See supplementary material at http://dx.doi.org/10.1063/1.4921206 for the spin wave dispersion profiles.
[24]O. Karlquist, Trans. R. Inst. Technol. Stockholm **86**, 3 (1954).
[25]S. Sheshukova, E. Beginin, A. V. Sadovnikov, Y. Sharaevsky, and S. Nikitov, IEEE Magn. Lett. **5**, 1–4 (2014).
[26]E. Beginin, A. V. Sadovnikov, Y. Sharaevsky, and S. Nikitov, Solid State Phenom. **215**, 389–393 (2014).
[27]P. Pirro, T. Brächer, A. V. Chumak, B. Lägel, C. Dubs, O. Surzhenko, P. Görnert, B. Leven, and B. Hillebrands, Appl. Phys. Lett. **104**, 012402 (2014).